Journal of Alloys and Compounds 542 (2012) 248–252

Contents lists available at SciVerse ScienceDirect

Journal of Alloys and Compounds

journal homepage: www.elsevier.com/locate/jalcom

Electrical resistometry study of an AlMgSi alloy under artificial aging

M. Stipcich [a,b,*], A. Cuniberti [a,b], V. Noseda Grau [a]

[a] IFIMAT, Instituto de Física de Materiales Tandil, Facultad de Ciencias Exactas, UNCentro, Pinto 399 (7000) Tandil, Argentina
[b] Consejo Nacional de Investigaciones Científicas y Técnicas, Argentina

ARTICLE INFO

Article history:
Received 26 March 2012
Received in revised form 5 July 2012
Accepted 6 July 2012
Available online 16 July 2012

Keywords:
AlMgSi alloy
β″ precipitation
Electrical resistometry
Vickers microhardness
Differential scanning calorimetry

ABSTRACT

The artificial aging of an AlMgSi commercial alloy was studied by electrical resistometry measurements. A laboratory-made experimental arrangement was designed in order to avoid natural aging prior to artificial aging. The electrical resistometry evolution was compared to Vickers microhardness determinations, and correlated with the precipitation sequence. The temporal evolution of β″ relative volume fraction is described by a normalized resistance evolution by means of a Johnson–Mehl–Avrami type equation. The activation energy is in good agreement with that obtained from differential scanning calorimetric experiments.

1. Introduction

Thermal treatment effects in precipitation hardened Al-based alloys require exhaustive studies in order to improve manufacturing routes and optimize the material performance. Because of their low density, good mechanical properties and corrosion resistance, Al–Mg–Si alloys belong to the most used structural materials. The precipitation process in these alloys has been studied for more than 50 years because of its primary role on the mechanical properties. There exists a high degree of accordance about the precipitation sequence during aging at intermediate temperatures, the so-called artificial aging (AA), which can be described as [1,2]:

$$\text{Al(SSS)} \rightarrow \text{GP zones} \rightarrow \beta'' \text{ precipitates} \rightarrow \beta' \text{ precipitates}$$

with Al(SSS)the supersaturated solid solution.

At the earlier times of AA, GP zones or pre-β″ phase are formed. These are spherical and fully coherent with the matrix, with Mg and Si content in a ratio close to 1. Pre-β″ evolves to β″ phase with the AA progress. β″ precipitates are nanometric, needle-shaped, and grow in one dimension, along Al ⟨100⟩, because of the small lattice mismatch in these directions with composition Mg_5Si_6 [1–3]. Following the AA, β′ phase, with hexagonal structure, is formed and grows [4]. Although the precipitation sequence has been extensively studied, the knowledge of the precipitation kinetics is still incomplete since it is affected by chemical composition, processing and/or aging practices.

One of the most common and useful experimental techniques for age-hardening evolution studies is the Vickers microhardness determination, Hμv. The typical behavior under AA consists of an Hμv increase up to a maximum value, underaging, followed by an Hμv decrease, overaging. Pre-β″ and β″ nucleation and growth govern the underaging stage. Overaging occurs once the β″ → β′ transformation takes place. Microhardness determinations are obtained at selected times along the isothermal curves, interrupting the AA treatment each time. This could be considered a disadvantage. Electrical resistivity (ER) measurement is an alternative technique [5–9], which allows examination of thermally activated processes without interruptions. While the versatility of the technique is known, it is not well established until now a quantitative evaluation of results.

The aim of this work is to present an approach for quantifying the pre-β″ and β″ phases evolution during AA of an AlMgSi commercial alloy monitored by electrical resistometry. The ER curves are compared to Hμv measurements, as well as with differential scanning calorimetry (DSC) results.

It is well known that solution-treated Al–Mg–Si alloys are prone to natural aging (NA). The Mg and Si clustering drastically changes the subsequent AA results [10–12]. Then, it is necessary to avoid the NA for AA studies. For this, a laboratory-made experimental arrangement was used, which minimizes the elapsed time between solution-quenching and ER measurements at the AA temperature.

* Corresponding author at: IFIMAT, Instituto de Física de Materiales Tandil, Facultad de Ciencias Exactas, UNCentro, Pinto 399 (7000) Tandil, Argentina. Tel.: +54 2293 439670; fax: +54 2293 439679.
E-mail address: mstipci@exa.unicen.edu.ar (M. Stipcich).

0925-8388/$ - see front matter © 2012 Elsevier B.V. All rights reserved.
http://dx.doi.org/10.1016/j.jallcom.2012.07.031

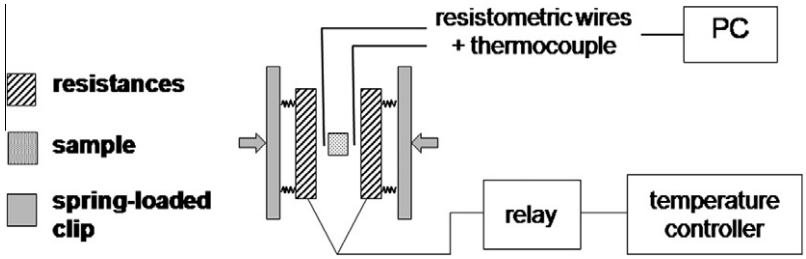

Fig. 1. Block diagram of the designed device for ER measurements.

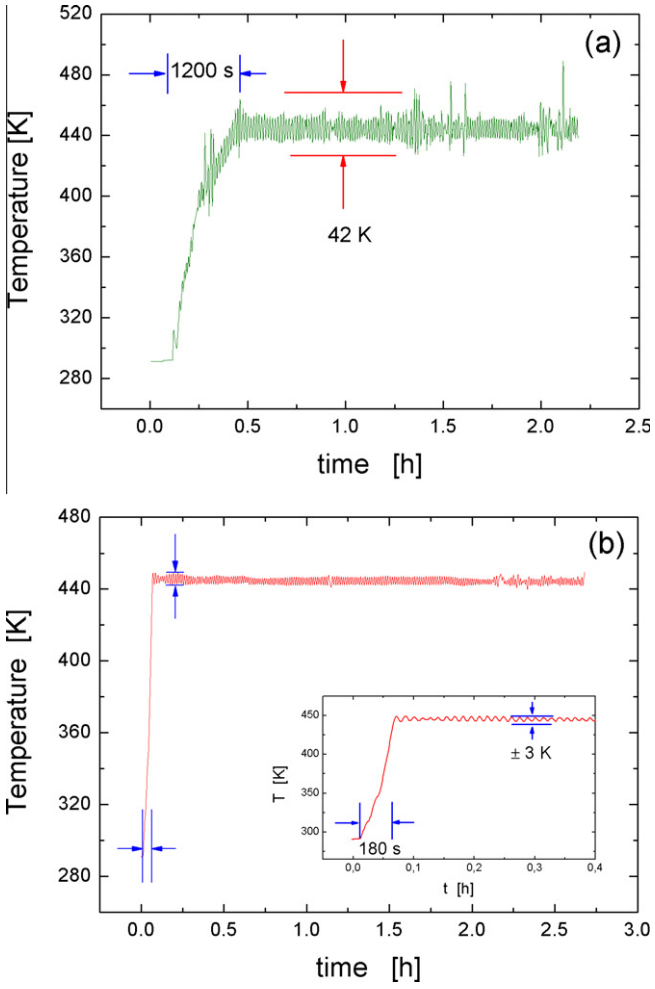

Fig. 2. Temperature–time record during a test at T_{AA} = 443 K in two temperature control conditions.

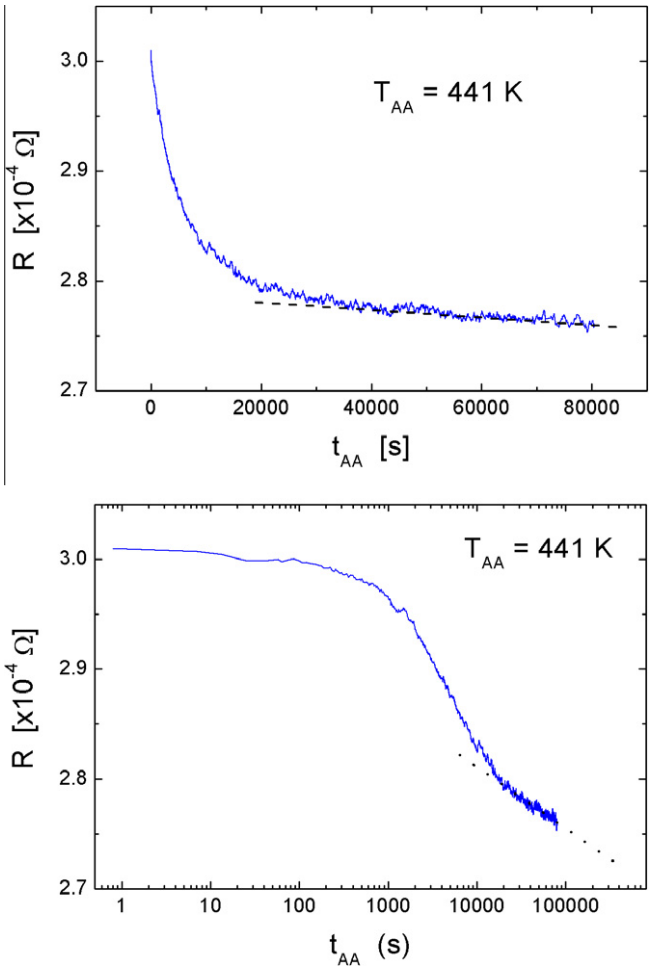

Fig. 3. Temporal evolution of electric resistance for T_{AA} = 441 K (linear and log scale). Dotted straight line is only eyes guide.

2. Experimental procedure

The studied material is a hot rolled commercial alloy supplied by Alcoa Europe, with composition Al–0.64 Mg–0.50Si–0.60Mn–0.05Cu–0.05Fe (%wt) determined with an emission spectrometer Metalscan 2000. Samples for electrical resistivity (ER) measurements were 30 mm long and (1.5 × 1.5) mm^2 cross-section. The laboratory-made arrangement for heating and ER measurement is described in the next section. ER measurements were performed using a four point probe system connected to a high accuracy Keithley current source and nanovoltimeter. The current passing through the material was ±100 mA. A Mitutoyo MVK-H11 for microhardness determinations and a Rheometric Scientific DSC SP differential scanning calorimeter were used.

3. Results and discussion

3.1. Electrical resistivity-furnace system

The designed system is shown in Fig. 1. The sample is placed between two small heating elements which operate as a coupled furnace. The heating elements are electrical resistances enveloped with mica. The four conductive wires (current and voltage) as well as the thermocouple (type K) are maintained in contact with the sample by means of a spring-loaded clip which press the heating elements. In this way, it is not necessary welding the wires to the sample. The system was introduced into a closed container

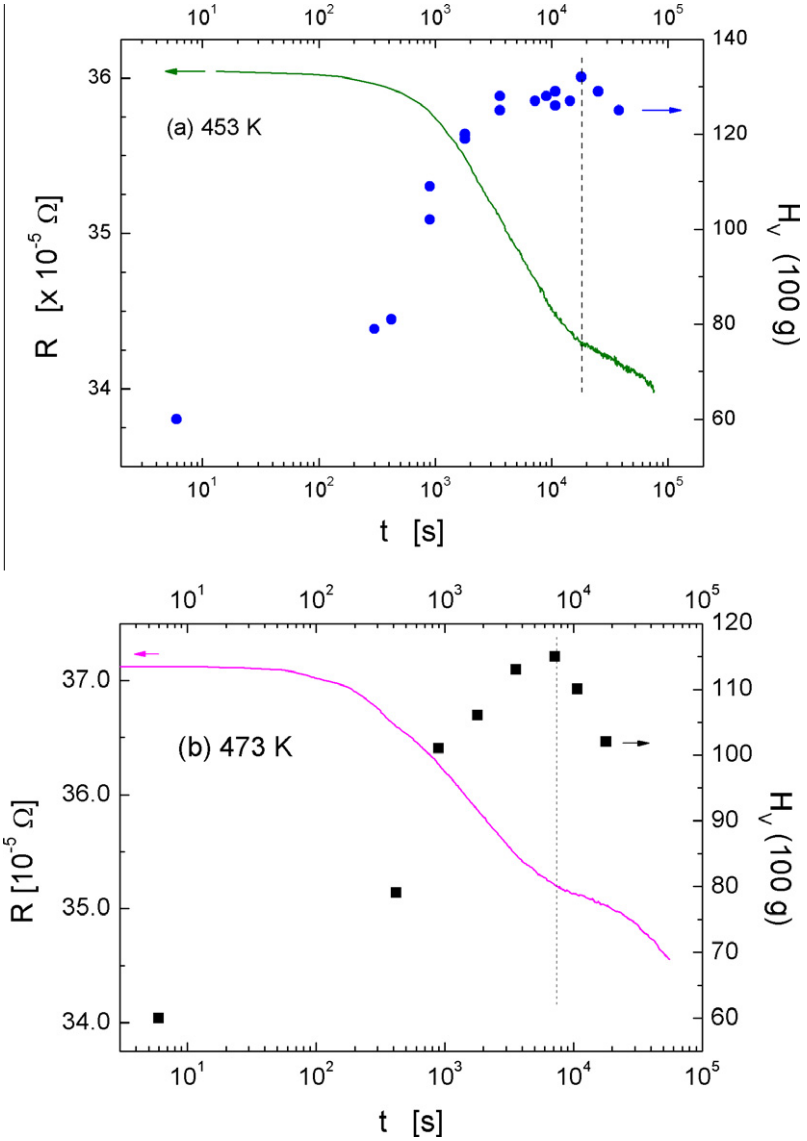

Fig. 4. Electrical resistance evolution against AA time (continuous line), and Vickers microhardness (●) for two temperatures. The experimental uncertainty in HμV is less than 10%.

during each experiment to reduce temperature fluctuations. The resistances are controlled by a solid state relay Autonics SPC1-50 with a cycle control output connected to analogical output of temperature controller NOVUS (PID) 1100. The temperature control was carefully calibrated in order to maximize the heating rate up to the AA temperature, and to ensure its stability. For these, it is fundamental to find an exact combination between the parameters *P*, *I* and *D* of the temperature controller, and the relay output controls. Fig. 2 shows the signal obtained in two calibration conditions. The condition of Fig. 2(b) is almost optimal considering the short heating time from room temperature up to the temperature T_{AA} and the reduced oscillation around T_{AA}.

3.2. Artificial aging test

The samples were subjected to a solution treatment at 823 K during 900 s and water quenched. Immediately after, the samples were positioned into the ER-furnace system, and subjected to AA. It was verified that the time necessary to reach the T_{AA} after quenching was less than 10 min for all the samples, avoiding NA. The AA temperatures were chosen in the range 430–480 K in order to promote the β″ precipitation.

The evolution of ER at a temperature T_{AA} = 441 K is shown in Fig. 3. In a linear *t*-scale, a sharp resistance decrease followed by an almost linear decrease with further aging is observed. Equivalently, in a log*t*-scale, the sharp resistance decrease ends with a slope change. In order to correlate the resistance evolution with the precipitation sequence, a comparison with microhardness determinations was made. The results obtained with both techniques are plotted in Fig. 4. It can be seen that the sharp ER decrease coincides with the Hμv increase stage, underaging, that is with the β″ precipitation stage. The ER slope change occurs almost simultaneously with the Hμv peak, indicating the overaging start. Then, it is plausible to identify the ER slope change with the beginning of the β″ → β′ transition. In this way, it is possible to identify the precipitation sequence from ER curves, particularly the β″ precipitation stage. There are no many ER plus Hμv results reported for the same alloy. However, it is worth noting that the peak strength time reported by Esmaeili et al. [13] also almost matches with the time at which the sharp ER decrease ends for AA at 453 K of a solution-treated AA6111 alloy [5].

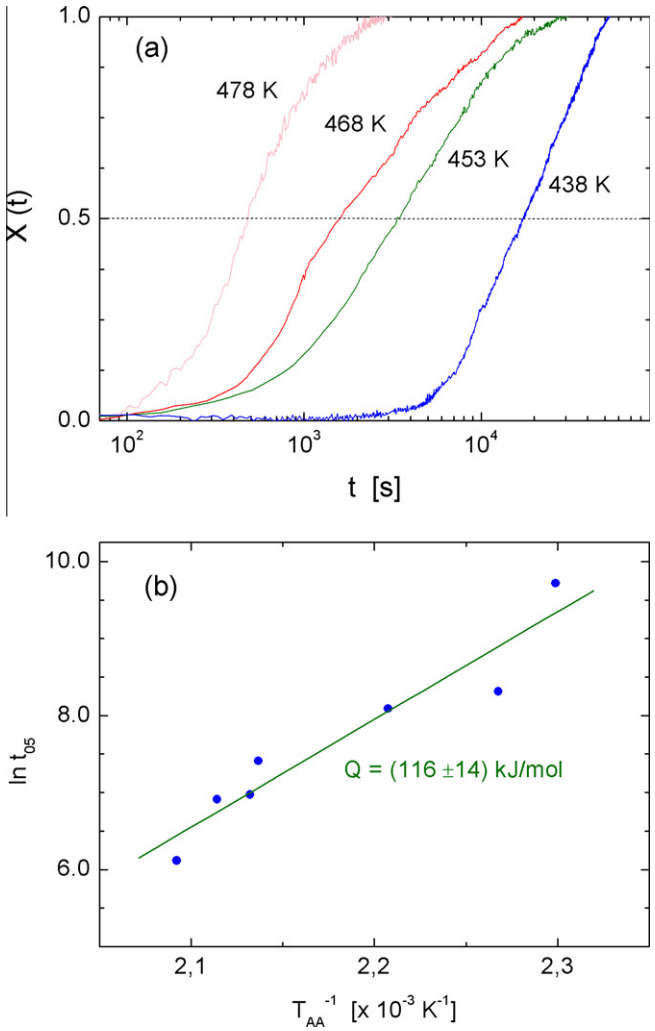

Fig. 5. (a) Time evolution of X(t) at different AA temperatures and (b) the Arrhenius plot.

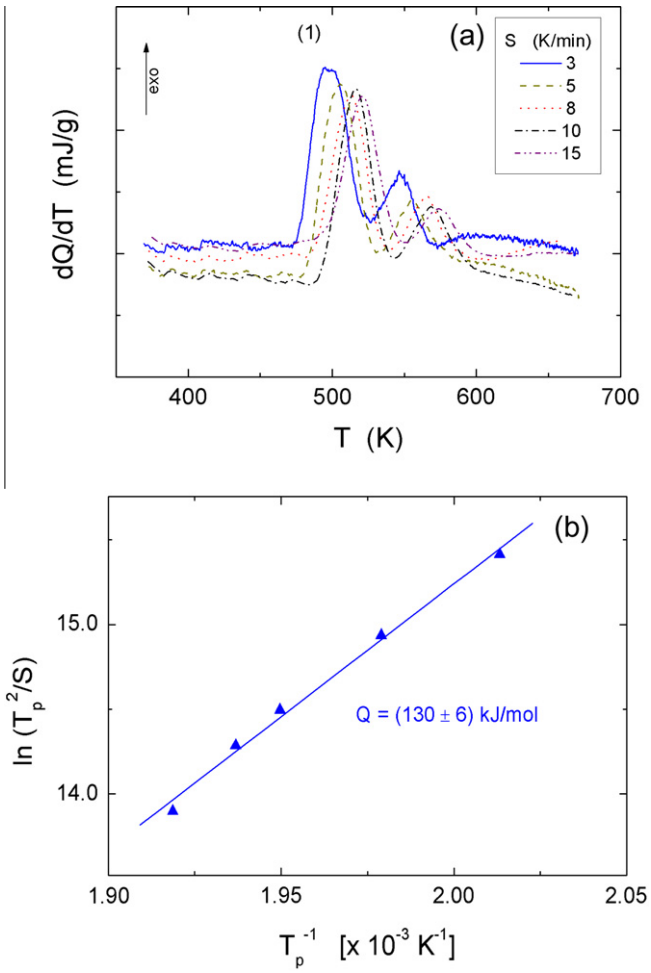

Fig. 6. (a) DSC cycles at different heating rates *S*. (b) Kissinger's plot (see text).

The difference in the resistance rate decrease with aging time can be associated with the gradual evolution of solute content in the matrix as precipitation proceeds. During underaging, the GP zones formation followed by β″ precipitation occurs, leading to an important matrix solute depletion up to the peak-aging. Then, the fast ER decrease during underaging can be linked to the decrease of Mg and Si in SS. It should be mentioned that according to data given in [14], the electrical resistivity changes $-0.32\ 10^{-8}\ \Omega$ m/wt.% for Mg out of SS, and $-0.93\ 10^{-8}\ \Omega$ m/wt.% for Si out of SS. The precipitates are already formed once overaging starts, and mainly transform from β″ to β′. Then, the solute depletion kinetics becomes slower and so the rate of resistance changes. This type of behavior has been observed in Al–Mg–Si alloys [5,6], and in other Al-based alloys like Al–Sc, because of the precipitation of Al_3Sc [15,16].

Based on those observations, and once the different *R*–*t* zones of the precipitations sequence are identified, a quantitative analysis of the β″ phase evolution can be made. The Johnson–Mehl–Avrami (JMA) formalism is commonly used for the description of nucleation and growth kinetic associated with hardness measurements [17,18], and also with resistivity measurements [15]. The temporal evolution of β″ relative volume fraction, $f_v(t)$, can be written as [19–21]:

$$f_v(t) = 1 - \exp(-K(T_{AA})t^n) \quad (1)$$

where $K(T_{AA})$ is a kinetics constant, and n is an exponent which characterizes the nature of nucleation and growth. The temperature dependence of $K(T_{AA})$ is modeled by an Arrhenius-type relationship, given by:

$$K(T_{AA}) = A\exp(-Q/RT_{AA}) \quad (2)$$

where A is a constant, Q is an activation energy, and R is the universal gas constant. The transformed fraction $X(t)$, proportional to $f_v(t)$, can be defined at each T_{AA} by a normalized resistance:

$$X(t) = \frac{[R(t=0) - R(t)]}{[R(t=0) - R(t_f)]} \quad (3)$$

where $R(t = 0)$ is the resistance at the start of the AA; and $R(t_f)$ is the resistance at the time of peak-aging, characterized by the slope change indicated by the dot line in Fig. 4. $X(t)$ varies between 0 and 1, assuming that at $t = 0$ and $t = t_f$ the relative volume fraction of β″ is 0 and 1, respectively.

Fig. 5(a) shows the evolution of $X(t)$ at different T_{AA}, with the typical sigmoidal form. From the slope of the straight zone an Avrami-exponent $n = 1.0 \pm 0.1$ was obtained. An exponent 1 corresponds to needles and plates of finite long dimension, small in comparison with their separation, or thickening of long cylinders (needles) [21]. This morphological description shows a good agreement with that observed in [12], for samples with identical chemical composition, which have been thermally treated at 453 K up to the peak aging condition.

The activation energy Q was obtained from the temperature dependence of the half time $t_{0.5}$, the time required to reach $f_v = 0.5$. Fig. 5(b) shows the Arrhenius plot, from which an activation energy $Q = (116 \pm 14)$ kJ/mol is obtained. It is worth noting that similar values of the time exponent n and the activation energy Q are obtained from the Hμv JMA analysis of the present alloy, and also have been obtained for other AlMgSi alloys [22–25].

In order to check the reliability of the ER analysis, the β″ precipitation was studied by differential scanning calorimetric (DSC) experiments, another well-established technique. Fig. 6(a) shows the thermograms obtained for heating rates $S = 3$, 5, 8, 10 and 15 K/min. Besides some controversies about the signals [13,26–28], there are strict coincidences about the identification of the peak indicated as (1) with the precipitation of β″ phase. The peak temperature T_p, at which the maximum heat flow is reached, increases with the scan rate increase.

For non-isothermal aging process, without any assumption of any specific kinetic model, an effective activation energy can be obtained by using the Kissinger's method [29,30]. From the dependence of the peak temperature T_p with the heating rate S, the activation energy is obtained by:

$$\ln\frac{S}{T_p^2} = -\frac{Q}{RT_p} - \ln\frac{Q}{RA} - \ln\beta_f \quad (4)$$

where β_f is a state variable, and A and R are the parameters used in the Arrhenius equation (3). The Kissinger's plot is presented in Fig. 6(b), and the resultant activation energy is $Q = (130 \pm 6)$ kJ/mol. This value is in good agreement with that obtained from the ER analysis, giving confidence in the ER determinations power for the quantitative evaluation of the β″ precipitation.

4. Conclusions

The AA phase transformations of an AlMgSi commercial alloy were studied by ER determinations. A laboratory-made experimental arrangement was designed in order to avoid NA previous to AA. The ER evolution was compared to Hμv determinations, and correlated with the precipitation sequence. The initial sharp resistance decrease is identified with the β″ precipitation zone, underaging, while the further almost linear ER decrease is identified with the β′ precipitation zone, overaging. The temporal evolution of β″ relative volume fraction, $f_v(t)$, is described by a normalized resistance evolution by means of a JMA type equation. The obtained activation energy is in good agreement with that obtained from differential scanning calorimetric (DSC) experiments. The proposed quantitative ER analysis allows monitoring the complete artificial aging process, with no interruptions as required in Hμv determinations.

Acknowledgments

This work was supported by ANPCYT, CONICET, and Secat-UNCentro, Argentina. The authors appreciate the helpful assistance of Technician Mr. O. Toscano.

References

[1] G.A. Edwards, K. Stiller, G.L. Dunlop, M.J. Couper, Acta Mater. 46 (1998) 3893–3904.
[2] M. Murayama, K. Hono, W.F. Miao, D.E. Laughlin, Metall. Mater. Trans. A 32 (2001) 239–246.
[3] H.W. Zandbergen, S.J. Andersen, J. Jansen, Science 277 (1997) 1221–1225.
[4] R. Vissers, M.A. van Huis, J. Jansen, H.W. Zandbergen, C.D. Marioara, S.J. Andersen, Acta Mater. 55 (2007) 3815–3823.
[5] S. Esmaeili, D.J. Lloyd, W.J. Poole, Mater. Lett. 59 (2005) 575–577.
[6] B. Raeisinia, W.J. Poole, D.J. Lloyd, Mater. Sci. Eng. A 420 (2006) 245–249.
[7] Shou-Yi Chang, Chi-Fang Chen, Su-Jien Lin, Theo Z. Kattamis, Acta Mater. 51 (2003) 6291–6302.
[8] W. Sha, Phys. Stat. Sol. (a) 202 (2005) 1903–1908.
[9] G. Riontino, M. Massazza, S. Abis, J. Mater. Res. 18 (2003) 1522–1527.
[10] C.D. Maioara, S.J. Andersen, J. Jansen, H.W. Zandbergen, Acta Mater. 51 (2003) 789–796.
[11] A. Serizawa, S. Hirosawa, T. Sato, Mater. Sci. Forum 519–521 (2006) 245–250.
[12] A. Cuniberti, A. Tolley, V. Castro Riglos, R. Giovachini, Mater. Sci. Eng. A 527 (2010) 5307–5311.
[13] S. Esmaeili, X. Wang, D.J. Lloyd, W.J. Poole, Metall. Mater. Trans. A 34 (2003) 751–763.
[14] J.E. Hatch, Aluminum: Properties and Physical Metallurgy, ASM, Metals Park, OH, 1984.
[15] J. Røyset, N. Ryum, Mater. Sci. Eng. A 396 (2005) 409–422.
[16] E. Clouet, A. Barbu, Acta Mater. 55 (2007) 391–400.
[17] W. Sha, Mater. Des. 28 (2007) 528–533.
[18] A.R. Eivani, A. Karimi Taheri, J. Mater. Proc. Technol. 205 (2008) 388–393.
[19] W.A. Johnson, R.F. Mehl, Trans. AIME 135 (1939) 416–442.
[20] M. Avrami, J. Chem. Phys. 7 (1939) 1103–1112.
[21] J.W. Christian, The theory of Transformations in Metals and Alloys, Pergamon Press, Oxford, 1975.
[22] S. Esmaeili, D.J. Lloyd, Acta Mater. 53 (2005) 5257–5271.
[23] L.C. Doan, Y. Ohmori, K. Nakai, Mater. Trans. JIM 41 (2000) 300–305.
[24] A. Gaber, A. Mossad Ali, K. Matsuda, T. Kawabata, T. Yamazaki, S. Ikeno, J. Alloys Compd. 432 (2007) 149–155.
[25] S. Pogatscher, H. Antrekowitsch, H. Leitner, T. Ebner, P.J. Uggowitzer, Acta Mater. 59 (2011) 3352–3363.
[26] K. Matsuda, S. Ikeno, H. Matsui, T. Sato, K. Terayama, Y. Uetani, Metall. Mater. Trans. A 36 (2005) 2007–2012.
[27] W. Sha, Metall. Mater. Trans. A 35 (2004) 3012–3015.
[28] Y. Birol, Mater. Sci. Eng. A 391 (2005) 175–180.
[29] H.E. Kissinger, Anal. Chem. 29 (1957) 1702–1706.
[30] E.J. Mittemeijer, L. Cheng, P.J. Van der Schaaf, C.M. Brakman, B.M. Korevaar, Metall. Trans. A 17 (1988) 925–932.